Int. J. Electrochem. Sci., 6 **(2011)** 5802 - 5814

International Journal of
ELECTROCHEMICAL
SCIENCE
www.electrochemsci.org

Corrosion Behaviour of Mild Steel in Sulphuric Acid Solution in Presence of Ceftazidime

Ashish Kumar Singh[1, 2, *], *Sudhish Kumar Shukla*[1, 2], *M. A. Quraishi*[1]

[1] Department of Chemistry, North West University (Mafikeng Campus) South Africa
[2] Department of Chemistry, Institute of Technology, Banaras Hindu University, Varanasi 221 005 (India)
[*]E-mail: singhapc@gmail.com

Received: 20 September 2011 / *Accepted:* 18 October 2011 / *Published:* 1 November 2011

The corrosion inhibition properties of ceftadizime (CZD) for mild steel corrosion in H_2SO_4 solution were analysed by electrochemical impedance spectroscopy (EIS), potentiodynamic polarization and gravimetric methods. Mixed mode of adsorption (Physisorption and chemisorption) is proposed for the inhibition and the process followed the Langmuir adsorption isotherm. The mechanism of adsorption inhibition and type of adsorption isotherm were proposed from the trend of inhibition efficiency with temperature, E_a and ΔG^{o}_{ads}. Potentiodynamic polarization study clearly revealed that CZD acted as mixed type inhibitor. The experimental data showed a frequency distribution and therefore a modelling element with frequency dispersion behaviour and a constant phase element (CPE) have been used.

Keywords: Adsorption; corrosion; EIS; ceftazidime; mild steel

1. INTRODUCTION

The corrosion of steel is the most common form of corrosion, especially in acid solution. Sulphuric acid is also an important mineral acid with many uses in the same systems and leads the researchers to the study of the effect of the corrosion inhibitors [1–4]. Organic materials act as corrosion inhibitors according to their functional group, which are adsorbed on the metal surface. Most of the efficient inhibitors used in industry are organic compounds which mainly contain oxygen, sulphur, nitrogen atoms and multiple bonds in the molecule through which they are adsorbed on metal surface [5, 6]. Though the existing data show that numerous N-heterocyclic organic compounds have good anticorrosive activity, some of them are highly toxic to both human beings and environment. The safety and environmental issues of corrosion inhibitors arisen in industries has always been a global concern. Due to increasing environmental awareness and adverse effect of some chemicals, research

activities in recent times are geared towards developing cheap, non-toxic and environmentally safe corrosion inhibitors [7-11].

The present article is devoted to study ceftadizime (CZD) as corrosion inhibitor for mild steel in hydrochloric acid solution using electrochemical impedance spectroscopy (EIS), potentiodynamic polarization and weight loss techniques. The survey of literature reveals that it is a non-toxic compound (LD_{50} dose is 710 mg/kg in rats) [12].

Ceftadizime is a commercial name of (6R,7R,Z)-7-(2-(2-aminothiazol-4-yl)- 2-(2-carboxypropan-2-yloxyimino)acetamido)-8-oxo-3-(pyridinium-1-ylmethyl)-5-thia-1-aza-bicyclo[4.2.0] oct-2-ene-2-carboxylate. It is a third-generation cephalosporin antibiotic and does not contain any toxic metallic elements. The structure of ceftadizime (CZD) is shown in Fig. 1.

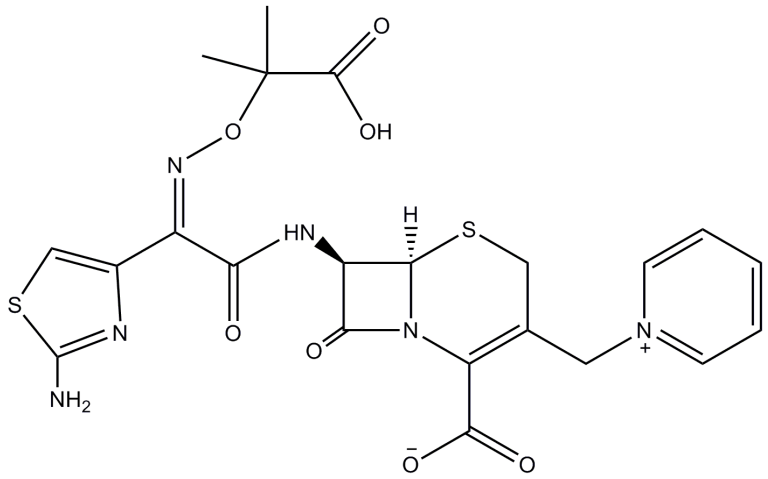

Figure 1. Structure of Ceftazidime molecule

2. EXPERIMENTAL

2.1 Inhibitor

Stock solution of CZD was made in 10:1 ratio water: ethanol mixture by volume to ensure solubility. This stock solution was used for all experimental purposes.

2.2 Corrosion measurements

Prior to all measurements, the mild steel specimens, having composition (wt %) C = 0.17, Mn= 0.46, Si = 0.26, S = 0.017, P = 0.019 and balance Fe, were abraded successively with emery papers from 600 to 1200 mesh/in grade. The specimen were washed thoroughly with double distilled water, degreased with acetone and finally dried in hot air blower. After drying, the specimen were placed in desiccator and then used for experiment. The aggressive solution of 0.5 M H_2SO_4 was prepared by dilution of analytical grade H_2SO_4 (98%) with double distilled water and all experiments were carried

out in unstirred solutions. The rectangular specimens with dimension 2.5 × 2.0 × 0.025 cm^3 were used in weight loss experiments and of size 1.0 × 1.0 cm^2 (exposed) with a 7.5 cm long stem (isolated with commercially available lacquer) were used for electrochemical measurements.

2.3 Electrochemical impedance spectroscopy

The EIS tests were performed at 308 ±1 K in a three electrode assembly. A saturated calomel electrode was used as the reference; a 1 cm^2 platinum foil was used as counter electrode. All potentials are reported versus SCE. Electrochemical impedance spectroscopy measurements (EIS) were performed using a Gamry instrument Potentiostat/Galvanostat with a Gamry framework system based on ESA 400 in a frequency range of 10^{-2} Hz to 10^5 Hz under potentiodynamic conditions, with amplitude of 10 mV peak-to-peak, using AC signal at E_{corr}. Gamry applications include software DC105 for corrosion and EIS300 for EIS measurements, and Echem Analyst version 5.50 software packages for data fitting. The experiments were carried out after 30 min. of immersion in the testing solution (no deaeration, no stirring).

The inhibition efficiency of the inhibitor was calculated from the charge transfer resistance values using the following equation:

$$\mu_{R_{ct}}\% = \frac{R_{ct}^{i} - R_{ct}^{0}}{R_{ct}^{i}} \times 100 \quad (1)$$

where, R_{ct}^{0} and R_{ct}^{i} are the charge transfer resistance in absence and in presence of inhibitor, respectively.

2.4 Potentiodynamic polarization

The electrochemical behaviour of mild steel sample in inhibited and non-inhibited solution was studied by recording anodic and cathodic potentiodynamic polarization curves. Measurements were performed in the 0.5 M H_2SO_4 solution containing different concentrations of the tested inhibitor by changing the electrode potential automatically from -250 to +250 mV versus corrosion potential at a scan rate of 1 mV s^{-1}. The linear Tafel segments of anodic and cathodic curves were extrapolated to corrosion potential to obtain corrosion current densities (i_{corr}).

The inhibition efficiency was evaluated from the measured i_{corr} values using the relationship:

$$\mu_{P}\% = \frac{i_{corr}^{0} - i_{corr}^{i}}{i_{corr}^{0}} \times 100 \quad (2)$$

where, i_{corr}^{0} and i_{corr}^{i} are the corrosion current density in absence and presence of inhibitor, respectively.

2.5 Weight loss measurements

Weight loss measurements were performed on rectangular mild steel samples having size 2.5 × 2.0 × 0.025 cm^3 by immersing the mild steel coupons into acid solution (100 mL) in absence and presence of different concentrations of CZD. After the elapsed time, the specimen were taken out, washed, dried and weighed accurately. All the tests were conducted in aerated 0.5 M H_2SO_4. All the experiments were performed in triplicate and average values were reported. From the evaluated weight loss, surface coverage (θ) was calculated using:

$$\theta = \frac{w_0 - w_i}{w_0} \qquad (3)$$

where, w_0 is weight loss in free acid solution and w_i is weight loss in acid solution in presence of inhibitor, respectively.

3. RESULTS AND DISCUSSION

3.1 Electrochemical impedance spectroscopy

Impedance method provides information about the kinetics of the electrode processes and simultaneously about the surface properties of the investigated systems. The shape of impedance gives mechanistic information.

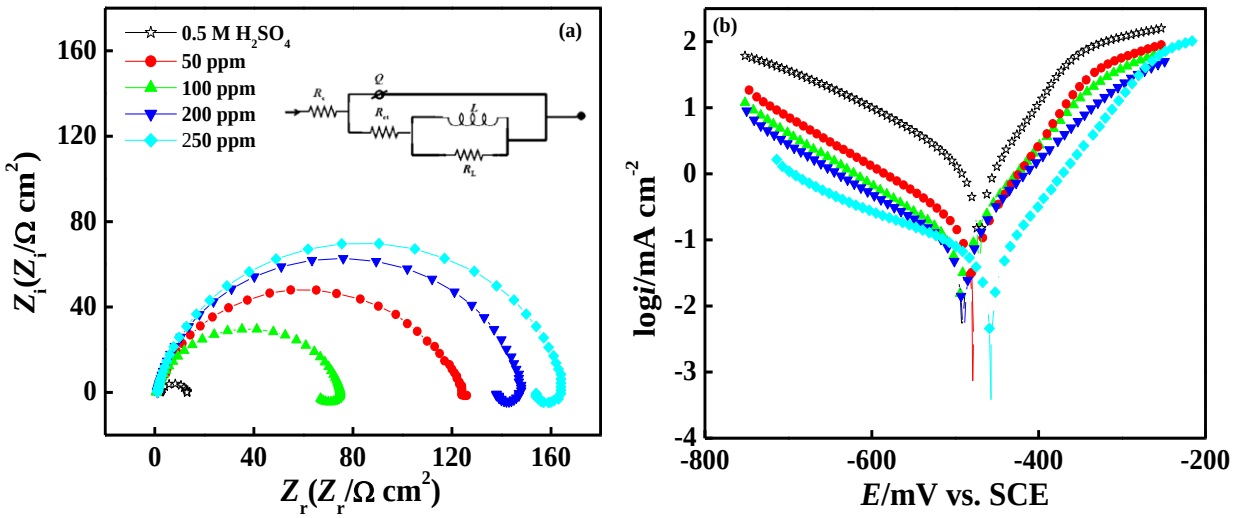

Figure 2. (a) Nyquist plots with equivalent circuit in insat and (b) Typical polarization curves of mild steel in 0.5 M H_2SO_4 in absence and presence of different concentrations of CZD

The method is widely used for investigation of the corrosion inhibition processes [13]. Nyquist plots of mild steel in 0.5 M H_2SO_4 solution in absence and presence of different concentrations of CZD are presented in Fig. 2a. It follows from Fig. 2a that a high frequency (HF) depressed charge-transfer semicircle was observed followed by a well defined inductive loop in the low frequency (LF) regions. The HF semicircle is attributed to the time constant of charge transfer and double-layer capacitance [14, 15]. The LF inductive loop may be attributed to the relaxation process obtained by adsorption species as $SO_{4\ ads}^{2-}$ and H_{ads}^{+} on the electrode surface [16].

To get more accurate fit of these experimental data, the measured impedance data were analysed by fitting in to equivalent circuit given in insat of Fig. 2a. The equivalent circuit consists of the double-layer capacitance (C_{dl}) in parallel to the charge transfer resistance (R_{ct}), which is in series to the parallel of inductive elements (L) and R_L. The presence of L in the impedance spectra in the presence of the inhibitor indicates that mild steel is still dissolved by the direct charge transfer at the CZD-adsorbed mild steel surface [6].

Table 1. Electrochemical parameters derived from EIS and potentiodynamic polarization in absence and presence of different concentrations of CZD

Inhibitor conc./ppm	EIS DATA				TAFEL DATA				
	R_{ct}/Ω cm^2	Y_0/Ω^{-1} s^n cm^{-2}	n	$\mu_{R_{ct}}$ %	$-E_{corr}$/mV vs. SCE	$i_{corr}/\mu A$ cm^{-2}	b_a/mV/dec	b_c/mV/dec	μ_p %
-	10.7	240	0.817	-	469	730	73	127	-
50	53.4	77	0.835	79.9	479	154	66	129	79.0
100	65.2	71	0.856	83.6	491	132	71	180	81.9
200	72.9	68	0.871	85.3	490	112	67	142	84.6
250	86.0	65	0.884	87.5	475	71	85	242	90.2

One constant phase element (CPE) is substituted for the capacitive element to give a more accurate fit, as the obtained capacitive loop is a depressed semi-circle. The depression in Nyquist semicircles is a feature for solid electrodes and often referred to as frequency dispersion and attributed to the roughness and other inhomogenities of the solid electrode [17]. The CPE is a special element whose admittance value is a function of the angular frequency (ω), and whose phase is independent of the frequency. The admittance and impedance of CPE is given by;

$$Y_{CPE} = Y_0(i\omega)^n \qquad (4)$$

where, Y_0 is the magnitude of CPE, i is an imaginary number ($i^2 = -1$) α is the phase angle of CPE and $n = \alpha/(\pi/2)$ in which α is the phase angle of CPE.

The point of intersection between the inductive loop and the real axis represents ($R_s + R_{ct}$). The electrochemical parameters, Including R_s, R_{ct}, R_L, L, Y_0 and n, obtained from fitting the recorded EIS using the electrochemical circuit of Fig 2a insat are listed in Table 1. C_{dl} values derived from CPE parameters according to equation (8) are listed in Table 1.

$$C_{dl} = Y_0(\omega_{max})^{n-1} \quad (5)$$

where, ω_{max} is angular frequency ($\omega_{max} = 2\pi f_{max}$) at which the imaginary part of impedance ($-Z_i$) is maximal and f_{max} is AC frequency at maximum.

3.2 Potentiodynamic polarization measurements

Polarization measurements were carried out in order to gain knowledge concerning the kinetics of the cathodic and anodic reactions. Fig. 2b presented the results of the effect of CZD concentration on the cathodic and anodic polarization curves of mild steel in 0.5 M H_2SO_4, respectively. It could be observed that both the cathodic and anodic reactions were suppressed with the addition of CZD, which suggested that the CZD reduced anodic dissolution and also retarded the hydrogen evolution reaction.

Electrochemical corrosion kinetics parameters, i.e. corrosion potential (E_{corr}), cathodic and anodic Tafel slopes (b_a, b_c) and corrosion current density (i_{corr}) obtained from the extrapolation of the polarization curves, were given in Table 1.

It followed from the Table 1 that the values of b_c changed with increasing inhibitor concentration, indicated the influence of the compounds on the kinetics of hydrogen evolution. The shift in the anodic Tafel slope b_c may be due to the chloride ions/or inhibitor molecules adsorbed onto steel surface. Due to the presence of some active sites, hetero-atoms in the studied compound for making adsorption, it may act as adsorption inhibitor. Being adsorbed on the metal surface, CZD controlled the anodic and cathodic reactions during corrosion process, and then its corrosion inhibition efficiency is directly proportional to the amount of adsorbed inhibitor. The functional groups and structure of the inhibitor play important roles during the adsorption process. On the other hand, an electron transfer may take place during adsorption of the neutral organic compounds at metal surface. Similar results were found by Ozcan et *al*. [18]. As it can be seen from Table 1, the studied inhibitor reduced both anodic and cathodic currents with a slight shift in corrosion potential (≈ 6-22 mV). According to Ferreira and others [19, 20], if the displacement in corrosion potential is more than 85 mV with respect to corrosion potential of the blank solution, the inhibitor can be seen as a cathodic or anodic type. In the present study, the maximum displacement was 22 mV which indicated that the studied inhibitor is a mixed type inhibitor. The results obtained from Tafel polarization showed good agreement with the results obtained from EIS.

3.3 Weight loss measurement

3.3.1 Effect of inhibitor concentration

Fig. 3a presented plot of inhibition efficiency *vs.* inhibitor concentration. From the Fig. 3a it can be seen that efficiency increased as the concentration increases. Hence, it can be concluded that at higher conc., availability of inhibitor increased to be adsorbed.

3.3.2 Effect of immersion time

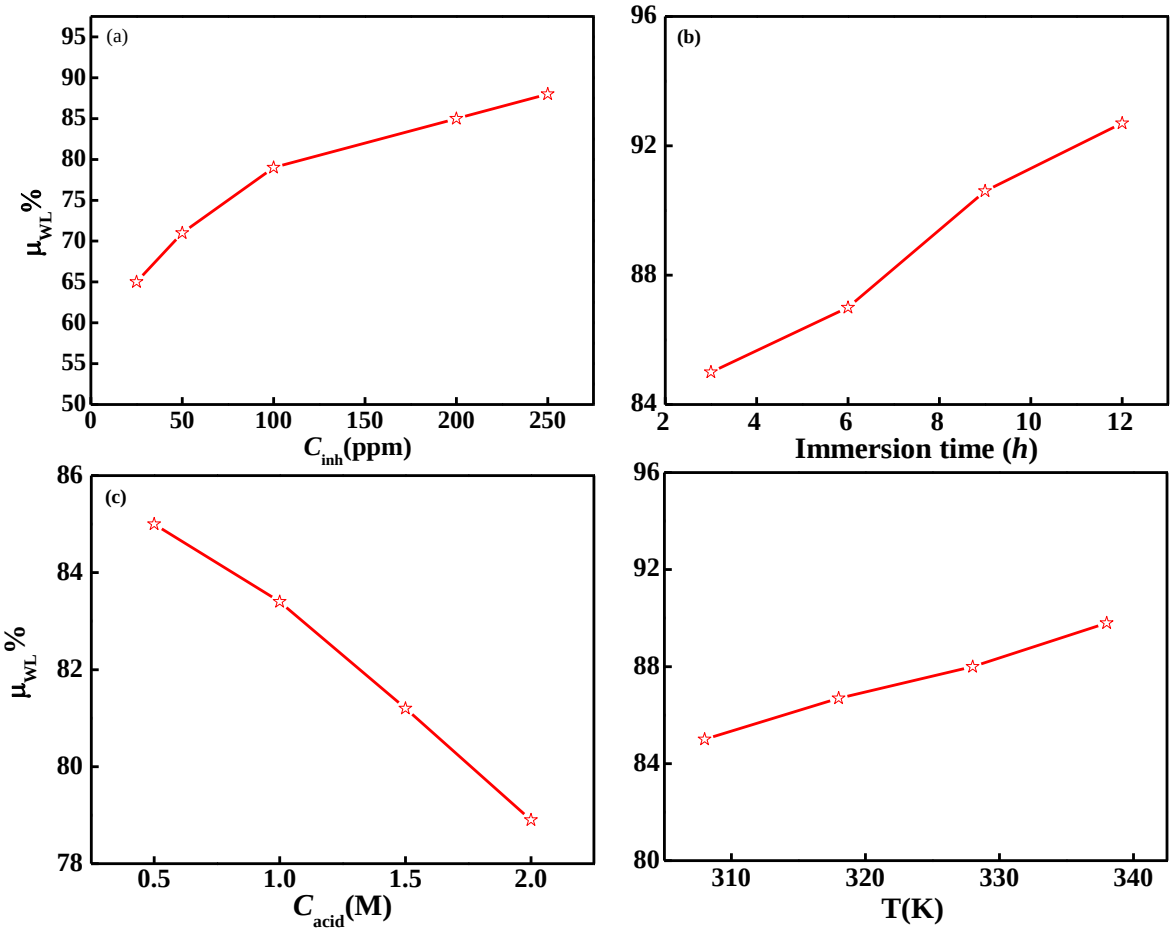

Figure 3. Plots of inhibition efficiency *vs.* (a) inhibitor conc., (b) immersion time, (c) acid concentration and (d) temperature of solution

From the Fig.3b, it can be seen that inhibition efficiency increased continuously with increasing immersion time. Thus, it can be concluded that persistent film formation is function of time.

3.3.1 Effect of acid concentration

The inhibition efficiency of CZD decreased 4-6% with increasing acid concentration from 0.5-2.0 M H_2SO_4 (Fig. 3c). Thus, CZD acted as effective inhibitor in the studied concentration range.

3.3.1 Effect of temperature of solution

The inhibition efficiency of CZD increased 4-5% with increasing temperature of solution from 308-338 K (Fig. 3d), indicated some chemical interaction of CZD with the metal surface.

3.4 Adsorption isotherm

Adsorption depends mainly on the charge and nature of the metal surface, electronic characteristics of the metal surface, adsorption of solvent and other ionic species, temperature of corrosion reaction and on the electrochemical potential at solution-interface. Adsorption of inhibitor involves the formation of two types of interaction responsible for bonding of inhibitor to a metal surface. The first one (physical adsorption) is weak undirected interaction and is due to electrostatic attraction between inhibiting organic ions or dipoles and the electrically charged surface of metal. The potential of zero charge plays an important role in the electrostatic adsorption process. The charge on metal surface can be expressed in terms of potential difference (ϕ) between the corrosion potential (E_{corr}) and the potential of zero charge (E_{pzc}) of the metal ($\phi = E_{corr} - E_{pzc}$). If ϕ is negative, adsorption of cations is favoured. On the contrary, the adsorption of anions is favourable if ϕ is positive. The second type of interaction (adsorption) occurs when directed forces govern the interaction between the adsorbate and adsorbent. Chemical adsorption involves charge sharing or charge transfer from adsorbates to the metal surface atoms in order to form a coordinate type of bond. Chemical adsorption has a free energy of adsorption and activation energy higher than physical adsorption and, hence, usually it is irreversible [21]. Adsorption isotherms are usually used to describe the adsorption process. The most frequently used isotherms include: Langmuir, Frumkin, Temkin, Flory-Huggins, Dhar-Flory-Huggins, Bockris-Swinkels and the recently formulated thermodynamic/kinetic model of El-Awady et al. [22, 23]. The establishment of adsorption isotherms that describe the adsorption of a corrosion inhibitor can provide important clues to the nature of the metal- inhibitor interaction. Adsorption of the organic molecules occurs as the interaction energy between molecule and metal surface is higher than that between the H_2O molecule and the metal surface [24].

In order to obtain the adsorption isotherm, the degree of surface coverage (θ) for various concentrations of the inhibitor has been calculated according to equation (3). Langmuir isotherm was tested for its fit to the experimental data. Langmuir isotherm is given by following equation:

$$\frac{C_{inh}}{\theta} = \frac{1}{K_{ads}} + C_{inh} \qquad (6)$$

where, K_{ads} is the equilibrium constant of the adsorption-desorption process, θ is the degree of surface coverage and C_{inh} is molar concentration of inhibitor in the bulk solution. The linear regression coefficient close to unity hence, adsorption of CZD followed Langmuir adsorption isotherm.

The enthalpy of adsorption can be calculated from the Gibbs–Helmholtz equation:

$$\left[\frac{\partial\left(\Delta G^{0}_{ads}/T\right)}{\partial T}\right]_{P} = -\frac{\Delta H^{0}_{ads}}{T^{2}} \qquad (7)$$

This equation can be arranged to following equation.

$$\frac{\Delta G^{o}_{ads}}{T} = \frac{\Delta H^{o}_{ads}}{T} + k \qquad (8)$$

The plot of $\Delta G^{0}_{ads}/T$ with *1 / T* gives a straight line with a slope that equals ΔH^{0}_{ads} (Fig. 4b). It can be seen from the Fig. 4b that $\Delta G^{0}_{ads}/T$ decreased with 1 / *T* in a linear fashion. The calculated values are depicted in Table 2. The negative sign of ΔH^{0}_{ads} in H_2SO_4 solution indicates that the adsorption of inhibitor molecule is an exothermic process. Generally, an exothermic adsorption process signifies either physic- or chemisorption while endothermic process is attributable unequivocally to chemisorption [25].

Table 2. Thermodynamic adsorption parameters for mild steel in presence of 200 ppm CZD

Inhibitor Conc./ppm	$-\Delta G^{o}_{ads}$ /kJ mol^{-1}	ΔH^{o}_{ads} /kJ mol^{-1}	ΔS^{o}_{ads} /J mol^{-1} K^{-1}
200	36.7	-17.8	61.3

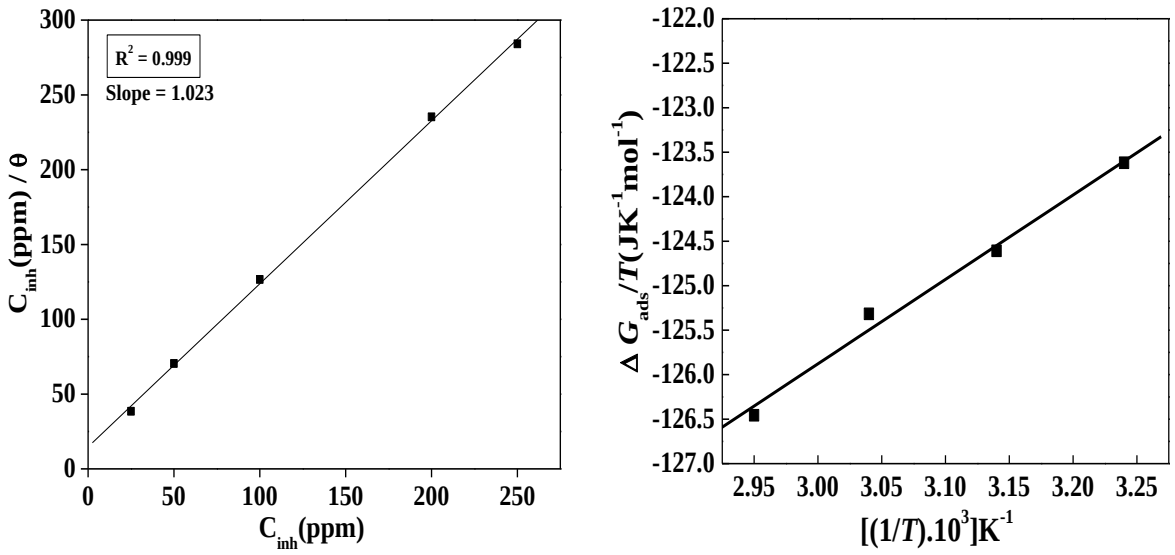

Figure 4. (a) Langmuir adsorption isotherm and (b) plot of $\Delta G^{0}_{ads}/T$ *vs.* 1/*T*

The sign of ΔH_{ads} is negative, hence, indicated that the adsorption of CZD is exothermic. As the value of ΔS^{0}_{ads} in Table 2, is positive in H_2SO_4 solution. This could be explained in the following way: the adsorption of CZD from the aqueous solution can be regarded as quasi-substitution process between the organic compound in the aqueous phase and water molecules at the mild steel surface

[26]. In this situation, the adsorption of CZD is accompanied by desorption of water molecules from the surface. Thus, as the adsorption of inhibitor is believed to be exothermic and associated with decrease in entropy of the solute, the opposite is true for solvent. Since, the thermodynamic values obtained are the algebraic sum of adsorption of organic inhibitor molecule and desorption of water molecules [27]. Therefore, gain in entropy is attributed to increase in solvent entropy. It means that in H_2SO_4 solution, driving force for the adsorption of adsorbate is the increase in entropy rather than the decrease in enthalpy.

3.8 Kinetic and thermodynamic considerations

The dependence of corrosion rate at temperature can be expressed by Arrhenius equation and transition state equation:

$$\log(C_R) = \frac{-E_a}{2.303RT} + \log\lambda \tag{9}$$

$$C_R = \frac{RT}{Nh}\exp\left(\frac{\Delta S^*}{R}\right)\exp\left(-\frac{\Delta H^*}{RT}\right) \tag{10}$$

where E_a apparent activation energy, λ the pre-exponential factor, ΔH^* the apparent enthalpy of activation, ΔS^* the apparent entropy of activation, h Planck's constant and N the Avogadro number, respectively. The apparent activation energy and pre-exponential factors for a 200 ppm of concentration of the inhibitor can be calculated by linear regression between $\log C_R$ and $1/T$, the results were shown in Table 3.

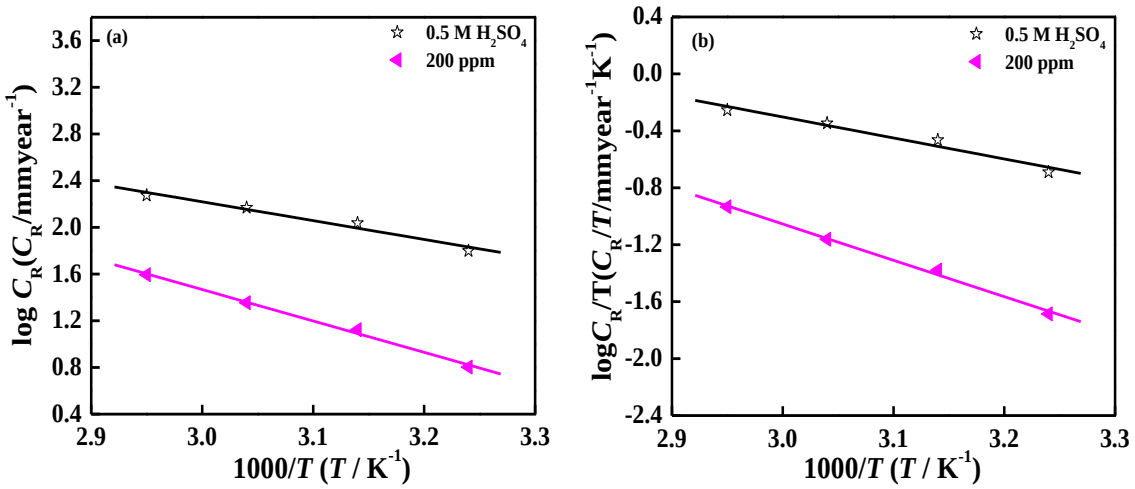

Figure 5. Adsorption isotherm plots in absence and presence of 200 ppm concentration of CZD for (a) log C_R *vs.* 1/*T*, (b) log (C_R/*T*) *vs.* 1/*T*

Fig. 5a depicted an Arrhenius plots for mild steel immersed in 0.5 M H_2SO_4 in absence and presence of 200 ppm concentration of CZD. The plots obtained are straight lines and the slope of each straight line gives its apparent activation energy. Table 3 presented E_a and λ values in absence and presence of 200 ppm concentration CZD.

According to equation (9), corrosion rate (C_R) is being affected by both E_a and λ. In general, the influence of E_a on the mild steel corrosion is higher than that of λ. However, if the variation in λ was drastically higher than that of E_a, the value of λ might be the dominant factor to determine the mild steel corrosion. In present case, E_a decreased and λ increased in presence of inhibitor (the higher E_a and lower λ led to lower corrosion rate). As it can be seen from Fig. 5a, the corrosion rate of steel decreased with increasing concentration; hence, it is clear that decrease in λ is the decisive factor affecting the corrosion rate of mild steel in 0.5 M H_2SO_4.

The relationship between $\log(C_R/T)$ and $1/T$ were shown in Fig. 5b. Straight lines are obtained with a slope $(-\Delta H^*/2.303R)$ and an intercept of $\left[\log(R/Nh)+(\Delta S^*/2.303R)\right]$, from which the value of ΔH^* and ΔS^* were calculated and presented in Table 3. The positive sign of enthalpy reflect the endothermic nature of steel dissolution process meaning that dissolution of steel is difficult. On comparing the values of entropy of activation (ΔS^*) listed in Table 3, it is clear that entropy of activation decreased in presence of the studied inhibitor compared to free acid solution. Such variation is associated with the phenomenon of ordering and disordering of inhibitor molecules on the mild steel surface. The decreased entropy of activation in the presence of inhibitor indicated that disorderness is decreased on going from reactant to activated complex.

4. MECHANISM OF INHIBITION

Generally, Corrosion inhibition mechanism in acid medium is the adsorption of inhibitor onto the metal surface. As far as the inhibition process is concerned, it is generally assumed that adsorption of the inhibitor at the metal/solution interface is the first step in the action mechanism of the inhibitors in aggressive acid media. Four types of adsorption may take place during inhibition involving organic molecules at the metal/solution inter-face: (1) electrostatic attraction between charged molecules and the charged metal, (2) interaction of unshared electron pairs in the molecule with the metal, (3) interaction of π-electrons with the metal, and (4) a combination of the above [28]. Concerning inhibitors, the inhibition efficiency depends on several factors; such as the number of adsorption sites and their charge density, molecular size, heat of hydrogenation, mode of interaction with the metal surface, and the formation metallic complexes [29]. Physical adsorption requires presence of both electrically charged surface of the metal and charged species in the bulk of the solution; the presence of a metal having vacant low-energy electron orbital and of an inhibitor with molecules having relatively loosely bound electrons or heteroatom with lone pair electrons. However, the compound reported can be protonated in an acid medium. Thus they become cations, existing in equilibrium with the corresponding molecular form:

$$CZD + xH^{+} \leftrightarrow [CZD_x]^{x+} \quad (11)$$

The protonated CZD, however, could be attached to the mild steel surface by means of electrostatic interaction between SO_4^{2-} and protonated CZD since the mild steel surface has positive charge in the H_2SO_4 medium [30]. This could further be explained based on the assumption that in the presence of SO_4^{2-}, the negatively charged SO_4^{2-} would attach to positively charged surface and thereby protonated CZD being adsorbed to the metal surface. Apart from electrostatic interaction, some chemical interaction is also involved. The non-bonding electrons of hetero atoms and π-electrons of aromatic ring caused chemical interaction.

5. CONCLUSIONS

The following main conclusions are drawn from the present study:

1. CZD was found to be a good inhibitor for mild steel corrosion in acid medium.

2. The increasing values of n indicated the decreasing roughness of mild steel surface with CZD concentration.

3. Potentiodynamic polarization study revealed that CZD acted as mixed type of inhibitor.

References

1. M. Benabdellah, A. Ousslim, B. Hammouti, A. Elidrissi, A. Aouniti, A. Dafali, K. Bekkouch, M. Benkaddour, *J. Appl. Electrochem*. 37 (2007) 819-826.
2. F. Bentiss, Mounim Lebrini, M. Traisnel, M. Lagrenee, *J. Appl. Electrochem*. 39 (2009) 1399–1407.
3. P.C. Okafor, M.E. Ikpi, I. E. Uwaha, E. E. Ebenso, U. J. Ekpe, S. A. Umoren, *Corros. Sci*. 50 (2008) 2310-2317.
4. L. Herrag, B. Hammouti, S. Elkadiri, A. Aouniti, C. Jama, H. Vezin, F. Bentiss, *Corros. Sci*. 52 (2010) 3042-3051.
5. A.K. Singh, M. A. Quraishi, *J. Appl. Electrochem.* 41 (2011) 7-18
6. A.K. Singh, M. A. Quraishi, *Mater. Chem. Phys*. 123 (2010) 666-677.
7. A.K. Singh, M. A. Quraishi, *Corros. Sci*. 52 (2010) 152-160.
8. M. S. Morad, *Corros. Sci*. 50 (2008) 436-448.
9. A.K. Singh, M. A. Quraishi, *Corros. Sci*. 52 (2010) 1529-1535.
10. O. K. Abiola, A.O. James, *Corros. Sci*. 52 (2010) 661-664.
11. F.S. de Souza, A. Spinelli, *Corros. Sci*. 51 (2009) 642-649.
12. K. Capel-Edwards, C. R. Losty, M. L. Tucker, D. A. H. Pratt, *J. Antimicrob. Chemother*. 8 (1981) Suppl. B, 237-239.
13. A.A. Hermas, M. S. Morad, M. H. Wahdan, *J. Appl. Electrochem*. 34 (2004) 95-102.
14. C. Deslouis, B. Tribollet, G. Mengoli, M. M. Musiani, *J. Appl. Electrochem*. 18 (1988) 374-383.
15. A.K. Singh, M. A. Quraishi, *Corros. Sci*. 51 (2009) 2752-2760
16. A.K. Singh, M. A. Quraishi, *Corros. Sci.* 52 (2010) 1373-1385
17. A.K. Singh, M. A. Quraishi, J. *Appl. Chem*. 40 (2010) 1293-1306.
18. M. Mahadavian, M. M. Attar, *Corros. Sci*. 48 (2006) 4152-4157.

19. E. McCafferty, N. Hackerman, J. *Electrochem. Soc*. 119 (1972) 146-154.
20. A.K. Singh, M. A. Quraishi, *Corros. Sci.* 53 (2011) 1288-1297
21. M. Ozcan, I. Dehri, M. Erbil, *Appl. Surf. Sci*. 236 (2004) 155-164.
22. E. S. Ferreira, C. Giancomelli, F. C. Giacomelli, A. Spinelli, *Mater. Chem. Phys*. 83 (2004) 129-134.
23. W. H. Li, Q. He, C. L. Pei, B. R. Hou, J. *Appl. Electrochem*. 38 (2008) 289-295.
24. G. Trabanelli, in: Mansfeld F (Ed.), Corrosion mechanism, Mercel Dekker, New York, 2006.
25. B. Donnely, T.C. Downie, R. Grzeskowiak, H.R. Hamburg, D. Short, *Corros. Sci*. 18 (1978) 109.
26. A.K. Singh, S. K. Shukla, M. Singh, M. A. Quraishi, *Mater. Chem. Phys*. 129 (2011) 68-76.
27. V. Branzoi, F. Branzoi, M. Baibarac, *Mater. Chem. Phys*. 65 (2000) 288.
28. H. M. Bhajiwala, R. T. Vashi, *Bull. Electrochem*. 17 (2001) 441-448.
29. D. Schweinsberg, G. George, A. Nanayakkara, D. Steinert, *Corros. Sci*. 28 (1988) 33-42.
30. A.Fouda, M. Moussa, F. I. Taha, A. I. ElNeanaa, *Corros. Sci*. 26 (1986) 719-726.